Author Manuscript

Author Manuscript

Author Manuscript

Author Manuscript

HHS Public Access

Author manuscript

Brain Stimul. Author manuscript; available in PMC 2021 June 03.

Published in final edited form as:

Brain Stimul. 2021 ; 14(1): 69–73. doi:10.1016/j.brs.2020.11.009.

White Matter Hyperintensities Affect Transcranial Electrical Stimulation in the Aging Brain

Aprinda Indahlastari, Ph.D.[1,2,†], **Alejandro Albizu, B.S.**[1,3], **Emanuel M. Boutzoukas, M.S.**[1,2], **Andrew O'Shea, M.Sc.**[1,2], **Adam J. Woods, Ph.D.**[1,2,3]

[1]Center for Cognitive Aging and Memory, McKnight Brain Institute, University of Florida, Gainesville, FL

[2]Department of Clinical and Health Psychology, College of Public Health and Health Professions, University of Florida, Gainesville, FL

[3]Department of Neuroscience, College of Medicine, University of Florida, Gainesville, FL

Abstract

Background: White matter hyperintensities (WMH) are estimated to occur in greater than 63% of older adults over the age of 60 years. WMH identified in the T2-weighted FLAIR images can be combined with T1-weighted images to enhance individualized current flow models of older adults by accounting for the presence of WMH and its effects on delivered tES current in the aging brain.

Methods: Individualized head models were derived from T1-weighted images of 130 healthy older adults (mean=71years). Lesions segmented from FLAIR acquisition were added to individualized models. Current densities were computed in the brain and compared between models with and without lesions.

Main results: Integrating WMH into the models resulted in an overall decrease (up to 7%) in median current densities in the brain outside lesion regions. Changes in current density and total lesion volume was positively correlated (R^2=0.3, p<0.0001).

Conclusions: Incorporating WMH into individualized models may increase the accuracy of predicted tES current flow in the aging brain.

Keywords

tES; aging; white matter hyperintensity; finite element model

INTRODUCTION

White matter hyperintensities (WMH) or white matter lesions are anatomical alterations of white matter tissues indicative of reduced myelin, axonal atrophy, and small vessel ischemia

[†]**Please address correspondence to**: Aprinda Indahlastari, Ph.D., Department of Clinical and Health Psychology, University of Florida, Gainesville, FL, USA, Phone: (352) 294-8631, aprinda.indahlas@phhp.ufl.edu.

AUTHOR DECLARATION

The authors report no conflicts of interest.

Author Manuscript Author Manuscript Author Manuscript Author Manuscript

that could lead to cognitive decline, cardiovascular diseases, and hypertension [1]. T2-weighted fluid-attenuated inversion recovery (FLAIR) is the most commonly use technique to detect WMH because of its sensitivity in capturing WMH contrast [2,3]. Prior research shows that WMH in older adults are associated with normal aging and the presence of WMH increases dramatically with age and various comorbid conditions [4,5]. The prevalence of WMH quantified from acquired T2-weighted images in healthy older adults over the age of 60 years were reported as high as 68– 95.83% [5–9].

Transcranial electrical stimulation (tES) applies mild current (1–2mA) to the scalp to improve brain functions and has shown promising results in older adults [10,11]. MRI-derived finite element models (FEM) have been used to predict tES current flow inside human's head and showed that individual brain morphology critically affects distributed current flow in the brain [12,13]. Given that the prevalence of WMH increases with age and the presence of WMH alters individual brain anatomy, WMH commonly found in older adults may affect tES current flow in the aging brain. In this study, we investigated the role of WMH on tES current flow in a large sample of healthy older adults (N=130). We incorporated WMH captured from T2-FLAIR imaging as lesion volumes (lesion FEM) into our previously constructed T1-derived FEM (non-lesion FEM) in an older adult population [14]. We hypothesized that increased fluid content within WMH in the brain would draw more current into the lesioned white matter regions and away from non-lesioned brain tissue. Therefore, we posited that the presence of WMH would result in less current delivered to intact gray and white matter.

METHODS

T1-weighted and FLAIR datasets in 130 healthy older adults (range:65–85, mean:71years) were utilized to create individualized FEM. Current density distribution in each brain was computed using an open source FEM software ROAST v2.7 [15]. Individual T1 data were segmented into 6 tissue types (CSF, bone, air, skin, white, and gray matter) and assigned conductivity values in ROAST [14]. Pad electrodes ($5\times7cm^2$) were added to the models with boundary conditions of 2mA applied at the anode (F4) and −2mA applied at the cathode (F3). Lesion maps were generated using an automated process in the Lesion Segmentation Toolbox [16]. At the beginning of the lesion generation process in the Lesion Segmentation Tool, the FLAIR data was co-registered to the T1 data resulting in the same resolution as the T1. Then, an algorithm consists of a binary classifier in the form of a logistic regression model trained on 53 MS patients was applied. Additionally, a similar lesion belief map was used as covariates for the lesion growth algorithm as well as spatial covariates that included voxelwise changes in lesion probability. The overall parameters of model fit were then utilized to estimate lesion probability for each voxel in new images, resulting in the lesion probability maps with resolution of $1mm^3$ [16]. The segmentation quality of individual lesion maps produced from the Lesion Segmentation Tool was visually inspected by overlaying the segmented lesions onto their respective FLAIR T2-weighted images. Further, regions with probability of 50% or higher in the lesion maps were binarized and added to segmented head models. Lesion volumes were assigned CSF conductivity values in ROAST [17,18]. Generated electric fields (EF,[Vm^{-1}]) were converted into current densities (J[Am^{-2}]) and compared to previously calculated Js in non-lesion FEM in our published study

Author Manuscript Author Manuscript Author Manuscript Author Manuscript

[14]. Percent differences of current density (PDJ) were computed between lesion and non-lesion FEM, within the brain tissue outside the lesion regions in the entire white and gray matter as well as within the superior frontal gyrus to represent target brain region [14]. Individual white matter and gray matter masks of the superior frontal gyrus were created based on the Desikan-Killiany atlas [19] in FreeSurfer v6.0 [20]. Total lesion volume (TLV) in each person generated from the toolbox [16] was correlated with computed PDJ. We computed a required current dose metric in each lesion FEM defined as the current dose required to achieve the same level of current dose in the brain as young adult brains from a 2mA stimulation [14]. The computed dosage was compared to previously calculated required dosage reported in our prior FEM study based on 2mA stimulation in 38 young adults (mean:27 years) [14].

RESULTS

Figure 1 shows the axial view of generated current density distribution within the brain to illustrate changes of current density pattern between lesion FEM (Figure 1A) and non-lesion FEM (Figure 1B). The subtraction of current density values in models with and without lesions is illustrated in Figure 1C. Overall, current density in the entire brain including lesion regions is found larger for lesion FEM (1A) than non-lesion FEM (1B), with large current concentrated in lesion location (1D). Regions with the most changes in current density values were found mostly in the white matter compartment, concentrated within and surrounding the lesions.

Calculated percentage differences in current density (PDJ) between lesion and non-lesion FEM within white matter, gray matter, and brain (white+gray matter) tissue are shown in Figure 2A. Maximum and minimum values for PDJ were found as 7.02% and −1.21%, respectively. Negative PDJs indicate that the brain region outside lesion location contained less current for the non-lesion FEM compared to lesion FEM. Positive correlation was observed between TLV and PDJ in white matter (R^2=0.355, p<0.0001), gray matter (R^2=0.074, p=0.0017), and white+gray matter (R^2=0.305, p<0.0001). The range of TLV was from 0.031mm^3 to 21mm^3. Computed current density within and nearby the superior frontal gyrus (SFG) as an example of target brain region is shown in Figure 2B with PDJs ranging from −1.69–11.38%. Positive correlations between TLV and PDJs of target region were found significant (p<0.0001) in white matter region surrounding the superior frontal gyrus (WM_SFG, $R^2_{WM\_SFG}$=0.486), gray matter within the superior frontal gyrus (GM_SFG, $R^2_{GM\_SFG}$=0.427), and combined regions ($R^2_{WM+GM\_SFG}$=0.531). Figure 2C shows the required current dose in the older adult cohort based on the averaged current dose in the young adult brain for lesion FEM (yellow) and non-lesion FEM (black). Figure 2C demonstrates no correlation found in the relationship between required current dose with age (C1), brain ratio (C2) and TLV (C3). Brain ratio was computed as the volume ratio of white +gray matter divided by total intracranial volume (white+gray+CSF). In general, current dose larger than 2mA is required to obtain the same current dose in the brain as those found in our previous young adult FEM as shown in Figure 2B. Current dose larger than those predicted in non-lesion FEM was required in lesion FEM to deliver equivalent 2mA stimulation to the rest of brain tissue outside the lesion region.

Author Manuscript Author Manuscript Author Manuscript Author Manuscript

DISCUSSION

This study is a follow up analysis to our previous tES modeling study [14] and, to the best of our knowledge, the largest tES modeling study that incorporated WMH detected in FLAIR to generate current density maps in an older adult cohort. Segmented WMH [16] were converted into binarized lesion volumes and added to the head models (lesion FEM). Changes in current density patterns (Figure 1) as well as computed percentage differences between current density values generated in lesion and non-lesion FEM (Figure 2A) demonstrated that WMH caused less current to be delivered to brain tissues outside the lesion regions. This observation provides insight into constructing a more accurate prediction of tES current flow and the potential need to adjust future tES application in older adults who exhibit WMH in their brains.

Overall, integrating WMH into FEM altered tES current distribution within the brain, and thus demonstrates the importance of incorporating WMH information to increase the accuracy of tES current flow prediction in older adults. We found at least 1 distinct WMH in all 130 healthy older adults within our sample (age 65–85), with total lesion volumes (TLV) ranging from 0.031 to 21.464 mm^3 (Figure 2A). This finding is consistent with prior research indicating WMH are highly prevalent and commonly found in healthy older adults [5]. Our results demonstrated that the presence of WMH significantly altered ($p<.0001$) the amount of current dose found in the brain tissue outside lesion regions by up to 7.02%, 3.36%, and 5.56% for white, gray matter, and white+gray matter tissue, respectively (Figure 2A). The difference in current dose was further increased in gray matter tissue within the superior frontal gyrus and nearby white matter regions outside the lesions. The superior frontal gyrus is part of the prefrontal cortex which is a stimulation target region for F3–F4 placement [14,21,22]. These findings suggest that WMH can affect current dose delivery in target regions and thus, when available, incorporating WMH information from the T2-weighted FLAIR images into segmented head volumes used in tES modeling may be necessary to produce a more accurate current flow prediction in healthy aging populations, or in other population with common white matter lesion occurrences e.g., multiple sclerosis, hypertension, etc. [16].

The effects of WMH on tES current delivery to the brain tissue outside the lesion regions might provide insight into future dose customization in older adults. The presence of WMH could either minimally or moderately alter current dose found in the brain depending on the lesion location. For instance, lesions located at the CSF boundary may cause a larger current decrease from the rest of the brain since CSF is highly conductive [14,23]. This observation is aligned with previous tES modeling studies that investigated the effects of stroke lesions on current distribution in the brain [17,18,24]. Further, comparison between generated current in the brain in lesion and non-lesion FEM (Figure 2B) indicated that the presence of WMH in the aging brain may require a slightly larger input current in order to achieve the same level of current dose equivalent to 2mA stimulation in young adults. Therefore, the present study provides critical information that can further improve existing prediction of tES current characteristics in older adults and a platform towards current dose customization for future tES applications in older adults.

Author Manuscript Author Manuscript Author Manuscript Author Manuscript

We acknowledge some limitations to the models presented in this study and recommend future studies to extend the application of our models. The FLAIR data used in our models were up sampled from 1×1×2.5mm to 1×1×1mm to generate lesion probability maps within the Lesion Segmentation Tool [16]. Future work should consider using FLAIR data that has resolution matching the T1 data e.g., $1mm^3$ to improve accuracy of segmented lesion regions. It should also be noted that any inaccuracy in segmented lesions would potentially alter current density distribution in non-lesioned brain regions. Therefore, the accuracy of lesion segmentation can be further verified by an expert such as a radiologist in future work. We assigned the lesioned regions with a high conductivity value that was equivalent to CSF. However, the assigned conductivity value was within the range of lesion conductivity values reported by McCann et al. and our model results were aligned with previous lesioned brain FEM studies in tES [13,17,24]. Future studies exploring assignment of a range of conductivity values to WMH based on characteristics of lesioned tissue may further improve the accuracy of FEM. Further, computed electric field strength within WMH regions had a maximum of 3.54V/m which is smaller than the electric field needed to cause pyramidal neurons to fire (28–79V/m) [25]. Therefore, stimulating brain regions with WMH presence should not induce an instant neuronal firing at the time of stimulation which agrees with previous tES literature [26]. However, the potential effects of current pooling within the lesion regions on neuronal firing warrant further research. In addition, findings reported in this study i.e., nominal changes in delivered current dose resulted from WMH presence will require further investigation in dose-response relationship that is crucial for refining the formulation of precision dosing applications in tES based on FEM. As WMH appear to alter the intensity of electric current induced within non-lesioned brain tissue, attempts to derive precision dosing approaches from FEM such as those that use machine learning [27] may underestimate the required dosing if WMH are not accounted for in models of older adult brain.

ACKNOWLEDGEMENTS

This work was supported in part by the National Institute of Aging/National Institutes of Health (K01AG050707, R01AG054077, T32AG020499), the National Heart, Lung, and Blood Institute (NHLBI)/National Institute of Health (T32HL134621), the Evelyn F. and William L. McKnight Brain Institute, and the McKnight Brain Research Foundation.

REFERENCES

[1]. Prins ND, Scheltens P. White matter hyperintensities, cognitive impairment and dementia: an update. Nat Rev Neurol 2015;11:157–65. doi:10.1038/nrneurol.2015.10. [PubMed: 25686760]

[2]. Bakshi R, Ariyaratana S, Benedict RHB, Jacobs L. Fluid-attenuated inversion recovery magnetic resonance imaging detects cortical and juxtacortical multiple sclerosis lesions. Arch Neurol 2001. doi:10.1001/archneur.58.5.742.

[3]. O'Shea AM, Woods AJ. White Matter Hyper-intensities. In: Gu D, Dupre ME, editors. Encycl. Gerontol. Popul. Aging, Cham: Springer International Publishing; 2019, p. 1–5. doi:10.1007/978-3-319-69892-2_684-1.

[4]. Yoshita M, Fletcher E, Harvey D, Ortega M, Martinez O, Mungas DM, et al. Extent and distribution of white matter hyperintensities in normal aging, MCI, and AD. Neurology 2006. doi:10.1212/01.wnl.0000249119.95747.1f.

Author Manuscript Author Manuscript Author Manuscript Author Manuscript

[5]. Ye Q, Chen X, Qin R, Huang L, Yang D, Liu R, et al. Enhanced regional homogeneity and functional connectivity in subjects with white matter hyperintensities and cognitive impairment. Front Neurosci 2019. doi:10.3389/fnins.2019.00695.

[6]. Zhuang FJ, Chen Y, He WB, Cai ZY. Prevalence of white matter hyperintensities increases with age. Neural Regen Res 2018. doi:10.4103/1673-5374.241465.

[7]. de Leeuw F-E. Prevalence of cerebral white matter lesions in elderly people: a population based magnetic resonance imaging study. The Rotterdam Scan Study. J Neurol Neurosurg Psychiatry 2001;70:9–14. doi:10.1136/jnnp.70.1.9. [PubMed: 11118240]

[8]. Lampe L, Kharabian-Masouleh S, Kynast J, Arelin K, Steele CJ, Löffler M, et al. Lesion location matters: The relationships between white matter hyperintensities on cognition in the healthy elderly. J Cereb Blood Flow Metab 2019. doi:10.1177/0271678X17740501.

[9]. Longstreth WT, Manolio TA, Arnold A, Burke GL, Bryan N, Jungreis CA, et al. Clinical Correlates of White Matter Findings on Cranial Magnetic Resonance Imaging of 3301 Elderly People. Stroke 1996;27:1274–82. doi:10.1161/01.STR.27.8.1274. [PubMed: 8711786]

[10]. Gomes-Osman J, Indahlastari A, Fried PJ, Cabral DLF, Rice J, Nissim NR, et al. Non-invasive Brain Stimulation: Probing Intracortical Circuits and Improving Cognition in the Aging Brain. Front Aging Neurosci 2018;10:177. doi:10.3389/fnagi.2018.00177. [PubMed: 29950986]

[11]. Hanley CJ, Alderman SL, Clemence E. Optimising cognitive enhancement: Systematic assessment of the effects of tdcs duration in older adults. Brain Sci 2020. doi:10.3390/brainsci10050304.

[12]. Indahlastari A, Chauhan M, Sadleir RJ. Benchmarking transcranial electrical stimulation finite element models: a comparison study. J Neural Eng 2019;16:026019. doi:10.1088/1741-2552/aafbbd. [PubMed: 30605892]

[13]. McCann H, Pisano G, Beltrachini L. Variation in Reported Human Head Tissue Electrical Conductivity Values. Brain Topogr 2019;32:825–58. doi:10.1007/s10548-019-00710-2. [PubMed: 31054104]

[14]. Indahlastari A, Albizu A, O'Shea A, Forbes MA, Nissim NR, Kraft JN, et al. Modeling transcranial electrical stimulation in the aging brain. Brain Stimul 2020;13:664–74. doi:10.1016/j.brs.2020.02.007. [PubMed: 32289695]

[15]. Huang Y, Datta A, Bikson M, Parra LC. Realistic vOlumetric-Approach to Simulate Transcranial Electric Stimulation -- ROAST -- a fully automated open-source pipeline. J Neural Eng 2019. doi:10.1088/1741-2552/ab208d.

[16]. Schmidt P, Gaser C, Arsic M, Buck D, Förschler A, Berthele A, et al. An automated tool for detection of FLAIR-hyperintense white-matter lesions in Multiple Sclerosis. Neuroimage 2012;59:3774–83. doi:10.1016/j.neuroimage.2011.11.032. [PubMed: 22119648]

[17]. Datta A, Baker JM, Bikson M, Fridriksson J. Individualized model predicts brain current flow during transcranial direct-current stimulation treatment in responsive stroke patient. Brain Stimul 2011;4:169–74. doi:10.1016/j.brs.2010.11.001. [PubMed: 21777878]

[18]. Wagner T, Fregni F, Fecteau S, Grodzinsky A, Zahn M, Pascual-Leone A. Transcranial direct current stimulation: A computer-based human model study. Neuroimage 2007;35:1113–24. doi:10.1016/j.neuroimage.2007.01.027. [PubMed: 17337213]

[19]. Desikan RS, Ségonne F, Fischl B, Quinn BT, Dickerson BC, Blacker D, et al. An automated labeling system for subdividing the human cerebral cortex on MRI scans into gyral based regions of interest. Neuroimage 2006. doi:10.1016/j.neuroimage.2006.01.021.

[20]. Fischl B FreeSurfer. Neuroimage 2012;62:774–81. doi:10.1016/j.neuroimage.2012.01.021. [PubMed: 22248573]

[21]. Gomes-Osman J, Indahlastari A, Fried PJ, Cabral DLF, Rice J, Nissim NR, et al. Non-invasive Brain Stimulation: Probing Intracortical Circuits and Improving Cognition in the Aging Brain. Front Aging Neurosci 2018;10. doi:10.3389/fnagi.2018.00177.

[22]. Nissim NR, O'Shea AM, Bryant V, Porges EC, Cohen R, Woods AJ. Frontal structural neural correlates of working memory performance in older adults. Front Aging Neurosci 2017;8. doi:10.3389/fnagi.2016.00328.

[23]. Mahdavi S, Towhidkhah F. Computational human head models of tDCS: Influence of brain atrophy on current density distribution. Brain Stimul 2018. doi:10.1016/j.brs.2017.09.013.

Author Manuscript Author Manuscript Author Manuscript Author Manuscript

[24]. Kalloch B, Bazin PL, Villringer A, Sehm B, Hlawitschka M. A flexible workflow for simulating transcranial electric stimulation in healthy and lesioned brains. PLoS One 2020. doi:10.1371/journal.pone.0228119.

[25]. Radman T, Ramos RL, Brumberg JC, Bikson M. Role of cortical cell type and morphology in subthreshold and suprathreshold uniform electric field stimulation in vitro. Brain Stimul 2009;2:215–228.e3. doi:10.1016/j.brs.2009.03.007. [PubMed: 20161507]

[26]. Chase HW, Boudewyn MA, Carter CS, Phillips ML. Transcranial direct current stimulation: a roadmap for research, from mechanism of action to clinical implementation. Mol Psychiatry 2020;25:397–407. doi:10.1038/s41380-019-0499-9. [PubMed: 31455860]

[27]. Albizu A, Fang R, Indahlastari A, O'Shea A, Stolte S, See KB, et al. Machine learning and individual variability in electric field characteristics predict tDCS treatment response. Under Rev 2020.

Author Manuscript Author Manuscript Author Manuscript Author Manuscript

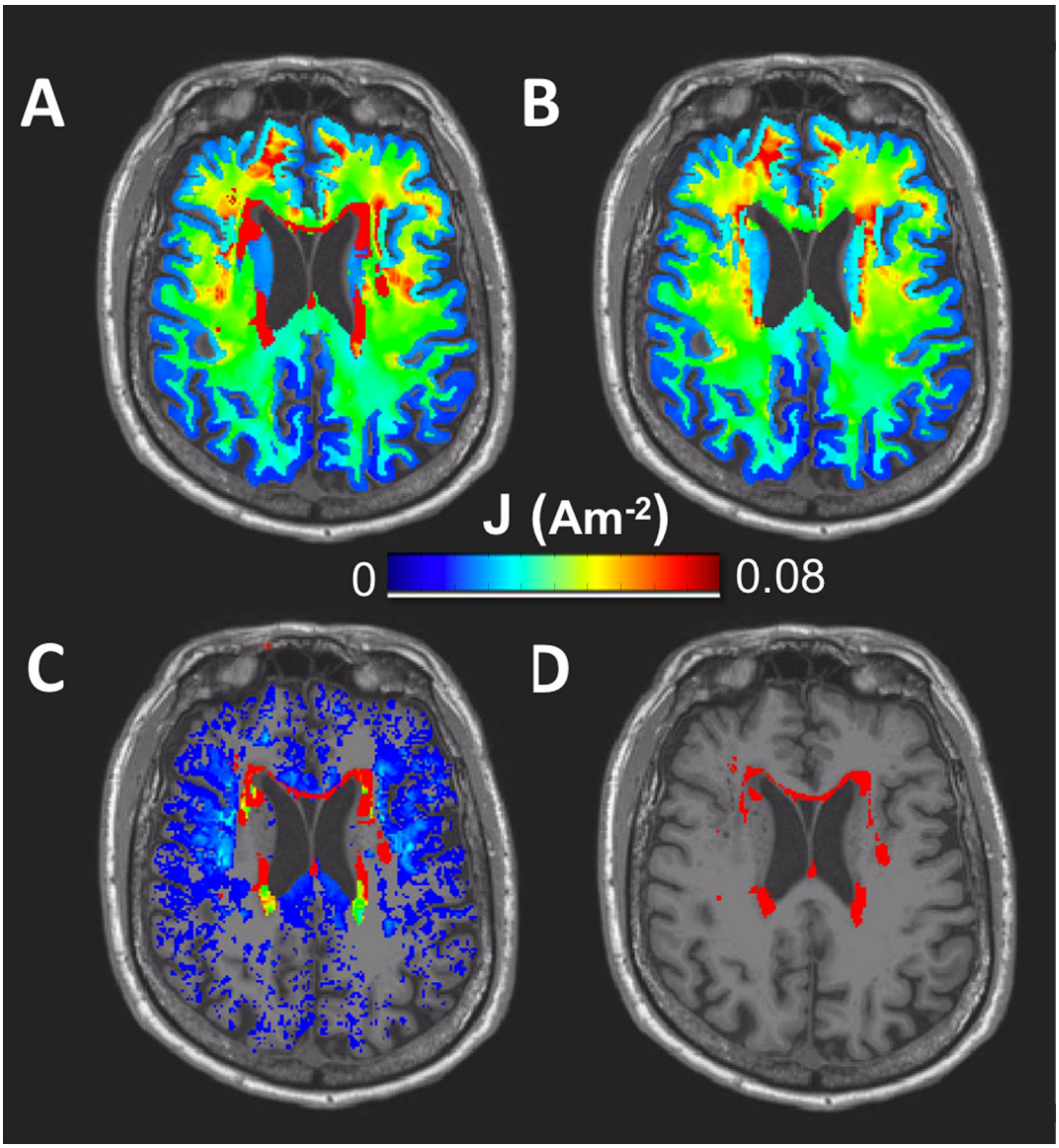

Figure 1.

Generated current density and lesion maps in the brain region (white and gray matter only). An axial view illustrates current density maps generated in **A)** lesion FEM **B)** non-lesion FEM, **C)** the subtraction of current density maps between lesion and non-lesion FEM, and **D)** location of the binarized lesion volume.

Author Manuscript Author Manuscript Author Manuscript Author Manuscript

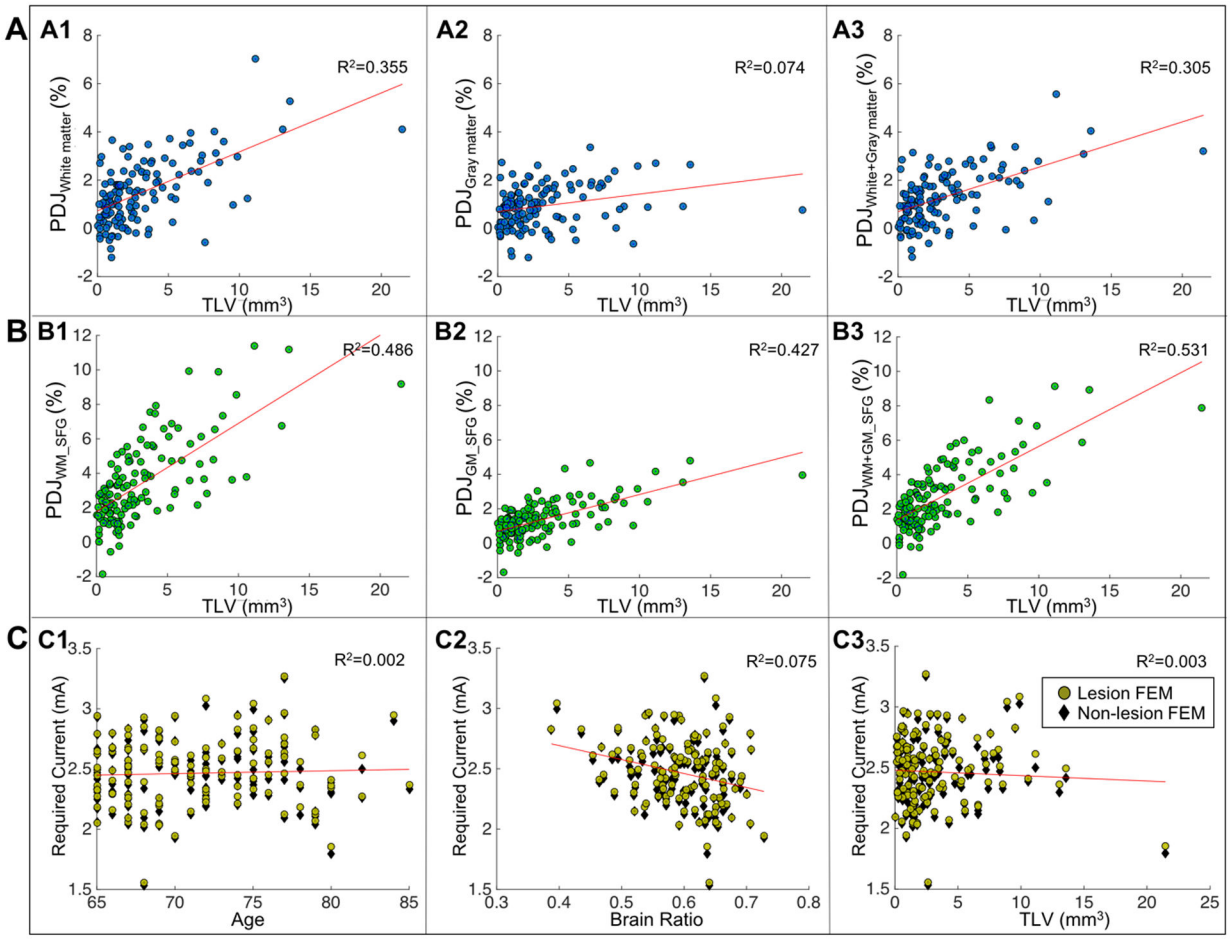

Figure 2.

Scatter plots of current density distribution in the brain. **A)** Correlation plots between total lesion volume (TLV) and percentage differences in current density (PDJ) in white matter (A1), gray matter (A2) and white+gray matter (A3). **B)** Correlation plots between total lesion volume (TLV) and percentage differences in current density (PDJ) within the superior frontal gyrus (SFG) for white matter SFG (B1), gray matter SFG (B2) and white+gray matter SFG (B3). **C)** Required current dose to be adjusted in the aging brain relative to a 2mA stimulation in young adult brains for lesion FEM (yellow circles) and non-lesion FEM (black diamonds) for dose vs. age (C1), dose vs. brain ratio (C2), and dose vs. TLV (C3).